A Potential Pulsar Halo: 1LHAASO J0635+0619

Chongyang Ren, Lingzhi Dong, Kun Fang, Jian Li, Zhe Li

Speaker: Chongyang Ren（任崇阳）

University of Science and Technology of China
Purple Mountain Observatory, CAS
Peking University
Institute of High Energy Physics, CAS

Outline

- Background
- LHAASO Observations and Results
- multi-wavelength observations
- Origin of multi-wavelength emisisons
- Summary

Background

Pulsar halos：
large-scale, low-density, and diffuse gamma-ray emissions surrounding middle-aged pulsars.

These halos are formed by the synchrotron radiation and inverse Compton scattering of electrons escaping from Pulsar Wind Nebulae (PWNe).

typically observed in the very-high-energy (VHE) and ultra-high-energy (UHE) gamma-ray bands.

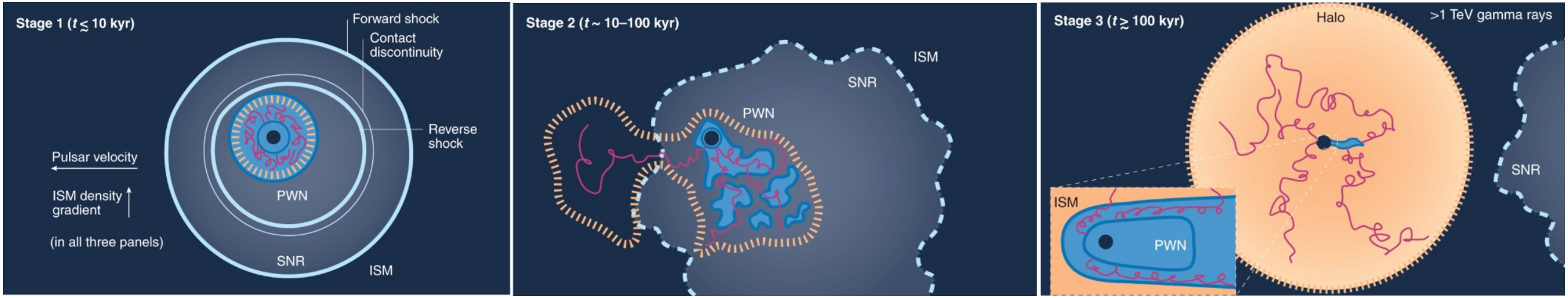

Ruben Lopez-Coto, et al., *Nature Astronomy*, 2022

Background

Current Pulsar halo and candidates.

Monogem

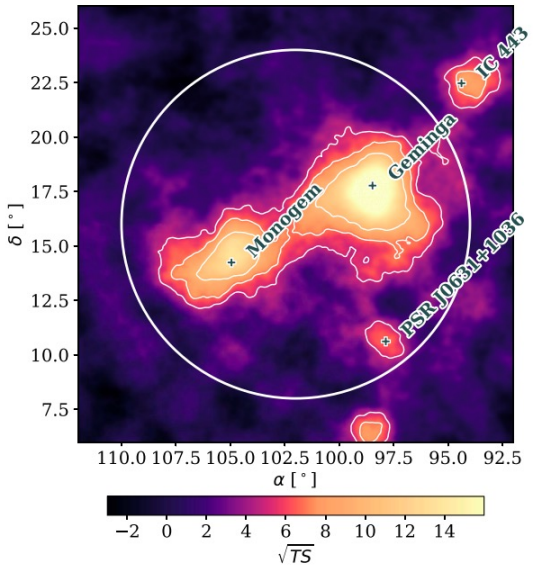

A. Abeysekara et al, 2017

PSR J0622+3749

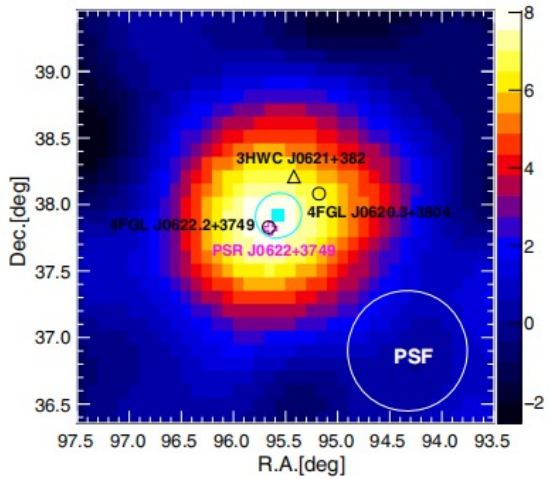

F. Aharonian et al, 2021

PSR J0248+6021

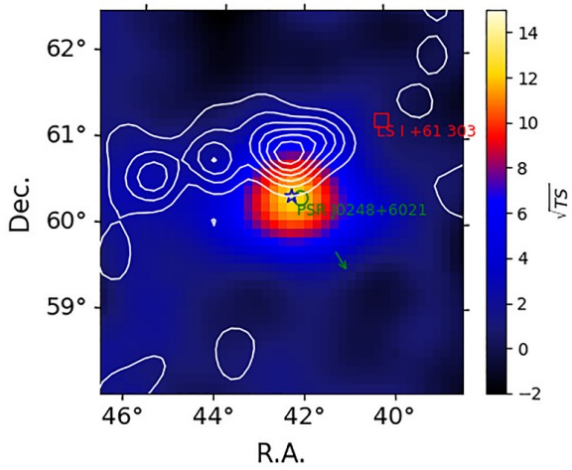

Z. Cao et al, 2025

PSR J0359+5414

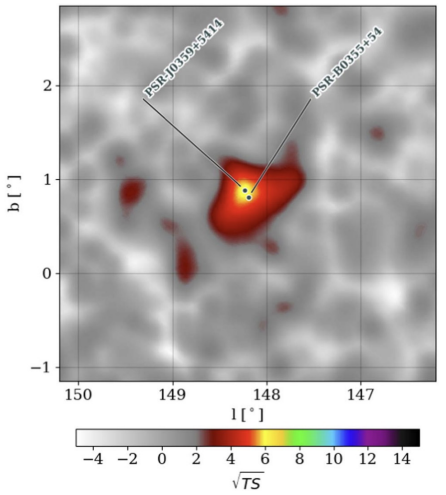

Albert et al, 2023

Background

Current Pulsar halo and candidates.

PSR B1055-52

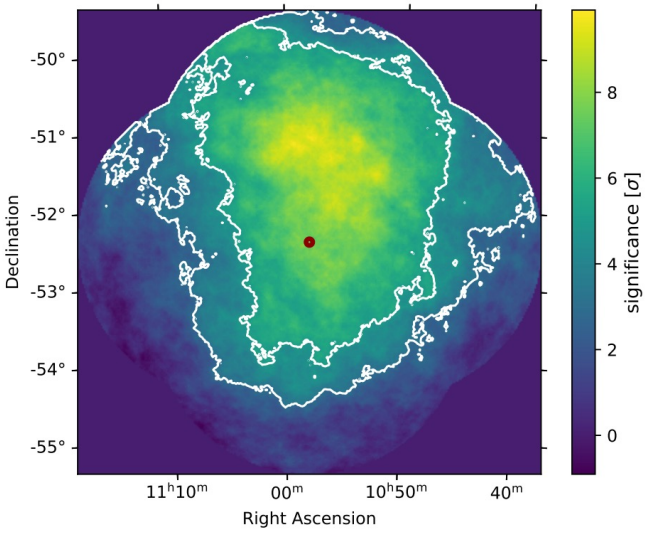

T. Wach et al., 2025

PSR J1831−0952

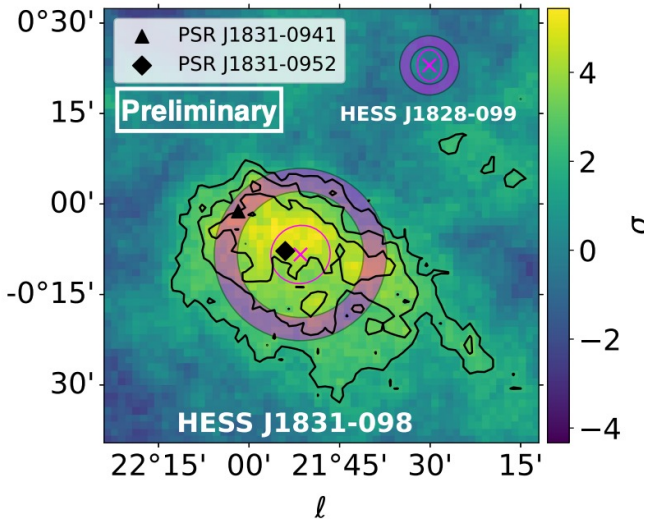

K. Sabri et al., 2025

PSR J1846+0919

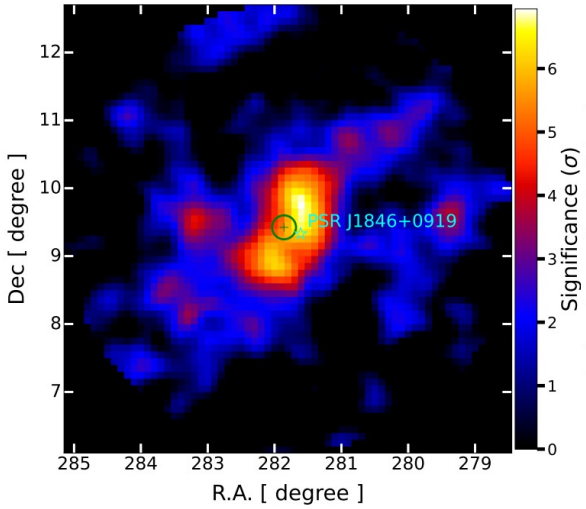

S. Hu et al., 2025

PSR J1813-1246

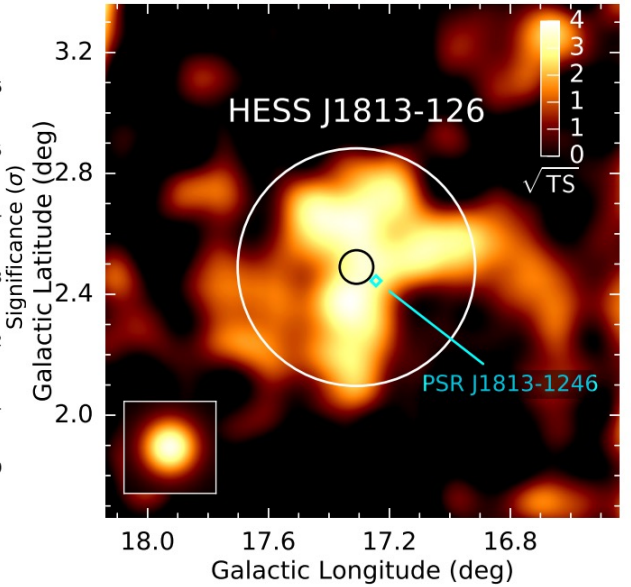

H.E.S.S. Collaboration et al., 2018

Background

1LHAASO J0635+0619 (or HAWC J0635 +070, J0635 here after) was detected as an extended very-high-energy gamma-ray source within the Monoceros Loop supernova remnant (G205.5+0.5) by LHAASO and HAWC.

This source exhibits characteristics suggestive of a pulsar halo of PSR J0633+0632.

PSR J0633+0632 is proposed to be associated with Monoceros Loop and the distance of the two obtained from different methods include 1.6 kpc (Odegard 1986; Borka Jovanovic & Urosevic), 1.98 kpc (Xiao & Zhu 2012), and 0.93 or 1.26 kpc (Yu et al. 2019).

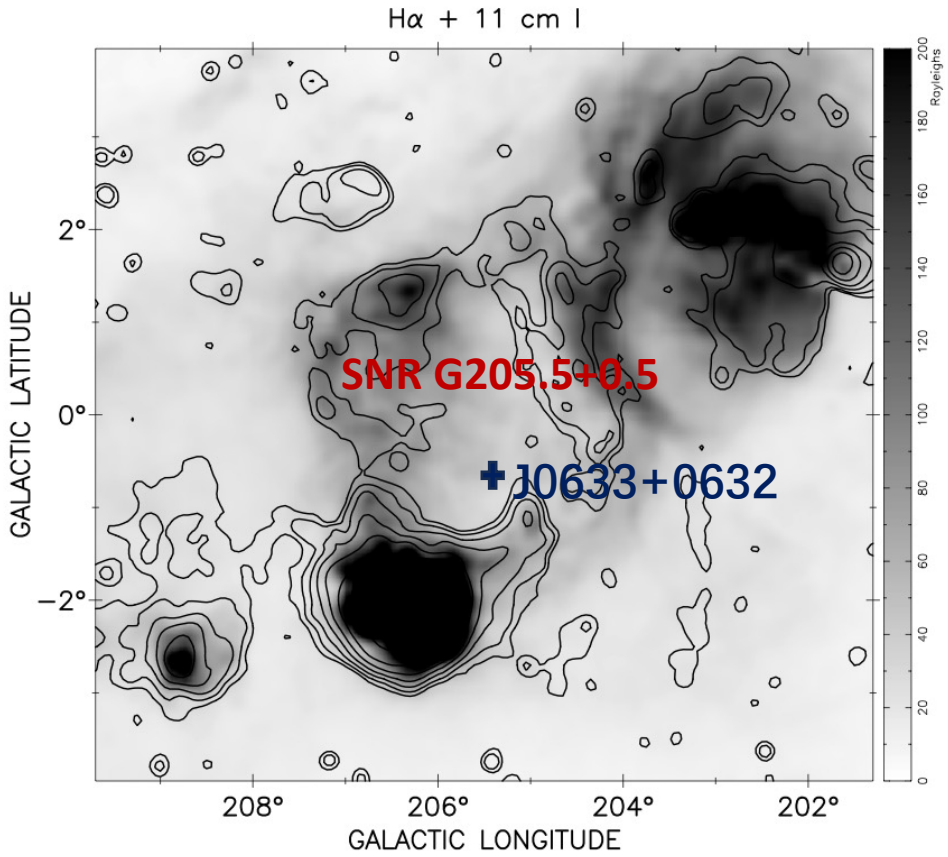

L. Xiao and M. Zhu, 2012

Background

Data Used:

- **ROI:** centered at (RA = 98.8°, Dec = 6.3°) with a radius of 6°
- **WCDA:** March 5, 2021 – July 31, 2025, livetime of 1484 days.
- **KM2A:** December 2019 – July 31, 2025, livetime of 1944 days.

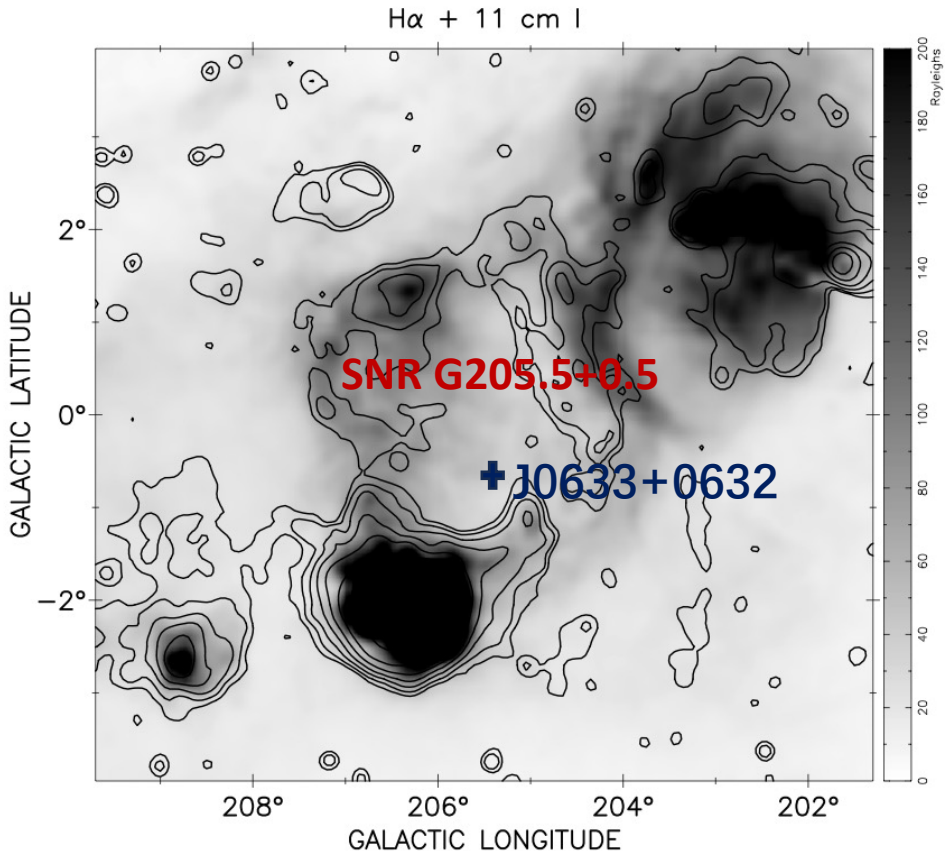

L. Xiao and M. Zhu, 2012

Data Analysis and Results

WCDA	RA (°)	Dec (°)	σ (°)	ΔTS
1 source	98.54 ± 0.08	6.42 ± 0.09	0.66 ± 0.08	0
2 Sources*	98.69 ± 0.11	6.66 ± 0.10	0.64 ± 0.10	40.48
	98.28 ± 0.04	5.80 ± 0.07	None	
3 Sources	98.68 ± 0.10	6.66 ± 0.10	0.64 ± 0.08	
	98.28 ± 0.05	5.79 ± 0.04	None	52.15
	100.47 ± 0.07	7.45 ± 0.07	None	
KM2A	**RA (°)**	**Dec (°)**	σ (°)	ΔTS
1 source*	98.67 ± 0.06	6.52 ± 0.06	0.52 ± 0.07	0
2 Sources	98.69 ± 0.02	6.52 ± 0.06	0.48 ± 0.06	9.63
	99.95 ± 0.09	6.37 ± 0.07	None	

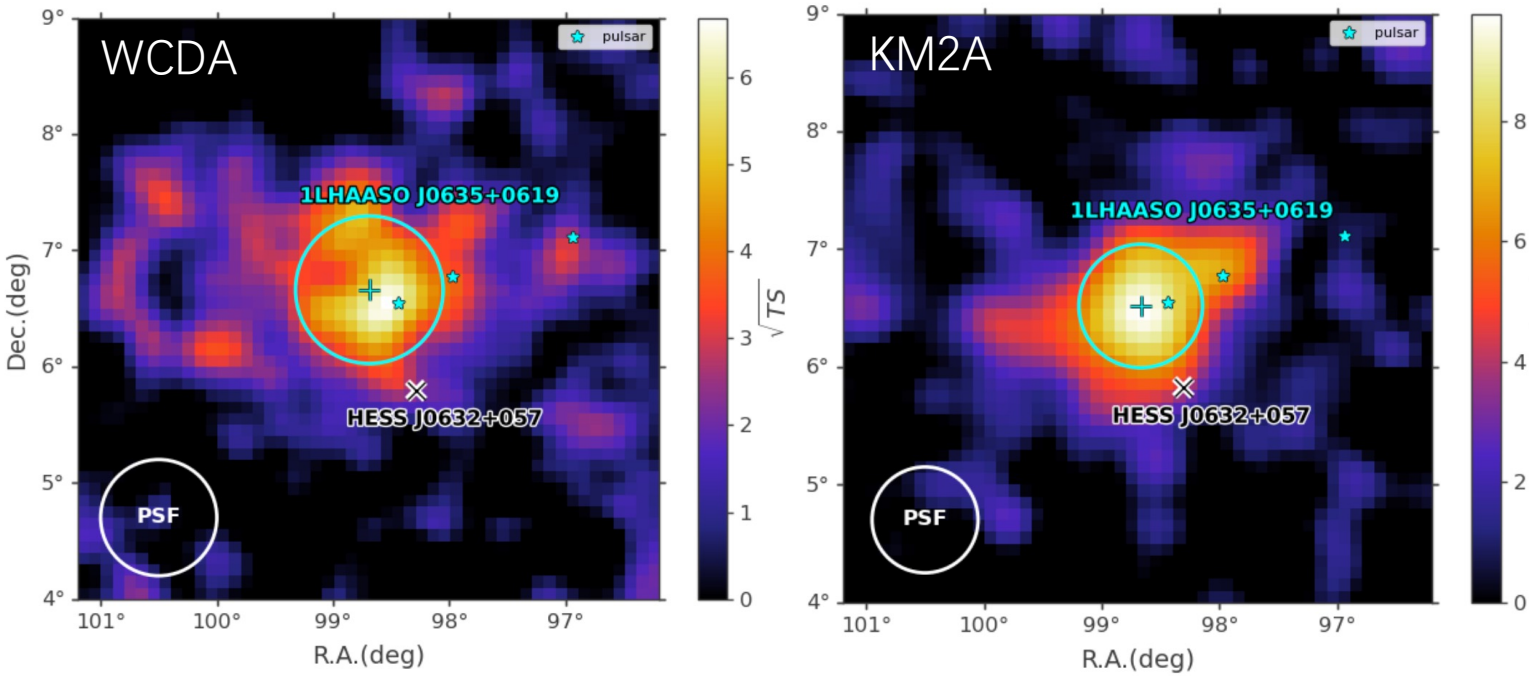

No significant detection ($< 5\sigma$) was observed in the significance sky maps at energies above 100 TeV.

Data Analysis and Results

We compared the results fitted by the halo and gaussian models.

$$f(\theta) \propto \frac{1}{\theta_d(\theta + 0.085\theta_d)} \exp\left[-1.54\,(\theta/\theta_d)^{1.52}\right]$$

Model	**RA (°)**	**Dec (°)**	**σ or θ_d (°)**	Flux[1)]	Index or α	E_{cut} or β	ΔAIC
Gaussian+LP	98.65 ± 0.05	6.57 ± 0.05	0.56 ± 0.05	0.79 ± 0.11	2.01 ± 0.17	1.20 ± 0.20	0
Gaussian+PLEC	98.65 ± 0.05	6.57 ± 0.05	0.56 ± 0.05	0.99 ± 0.19	1.62 ± 0.23	24.43 ± 6.41	-0.51
Diffusion+LP	98.64 ± 0.05	6.56 ± 0.04	1.82 ± 0.30	1.11 ± 0.23	2.08 ± 0.16	1.13 ± 0.19	-7.36
Diffusion+PLEC	98.63 ± 0.05	6.58 ± 0.04	1.84 ± 0.27	1.36 ± 0.23	1.77 ± 0.24	27.21 ± 9.09	-6.71

1) the pivot energy is 10 TeV, the unit is $10^{-14}\mathrm{TeV}^{-1}\,\mathrm{cm}^{-2}\,\mathrm{s}^{-1}$

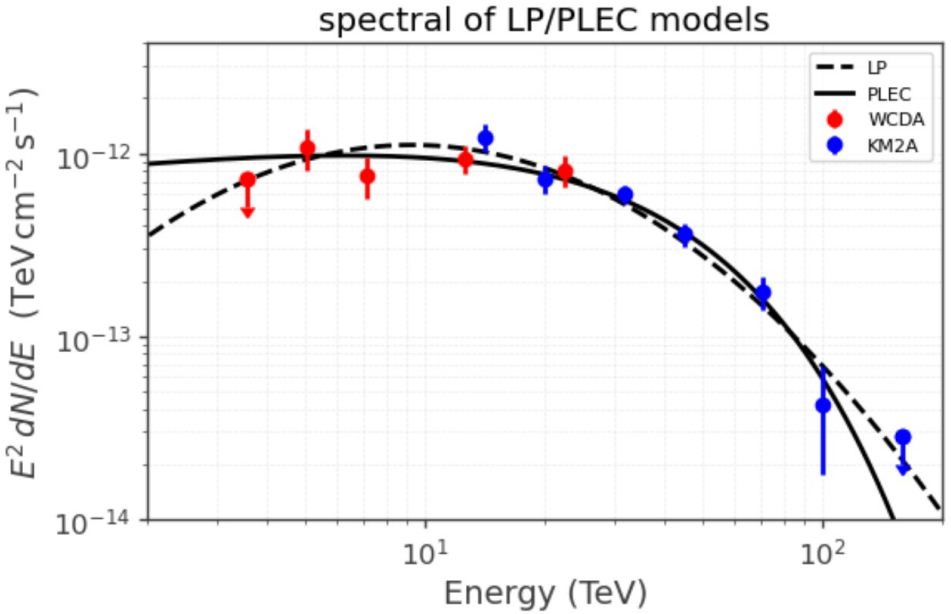

Data Analysis and Results

WCDA

Model	RA (°)	Dec (°)	σ or θ_d (°)	Flux[1)]	Index	ΔAIC
Gaussian	98.69 ± 0.11	6.66 ± 0.10	0.64 ± 0.10	0.57 ± 0.12	2.15 ± 0.12	0
Diffusion	98.64 ± 0.04	6.59 ± 0.03	2.12 ± 0.59	0.84 ± 0.30	2.19 ± 0.12	-0.90

1) the pivot energy is 10 TeV, the unit is $10^{-14}\mathrm{TeV}^{-1}\,\mathrm{cm}^{-2}\,\mathrm{s}^{-1}$

KM2A

Model	RA (°)	Dec (°)	σ or θ_d (°)	Flux[1)]	Index	ΔAIC
Gaussian	98.65 ± 0.06	6.57 ± 0.05	0.56 ± 0.05	1.25 ± 0.17	3.33 ± 0.08	0
Diffusion	98.63 ± 0.05	6.58 ± 0.03	1.83 ± 0.27	1.60 ± 0.30	3.32 ± 0.07	-4.28

1) the pivot energy is 10 TeV, the unit is $10^{-14}\mathrm{TeV}^{-1}\,\mathrm{cm}^{-2}\,\mathrm{s}^{-1}$

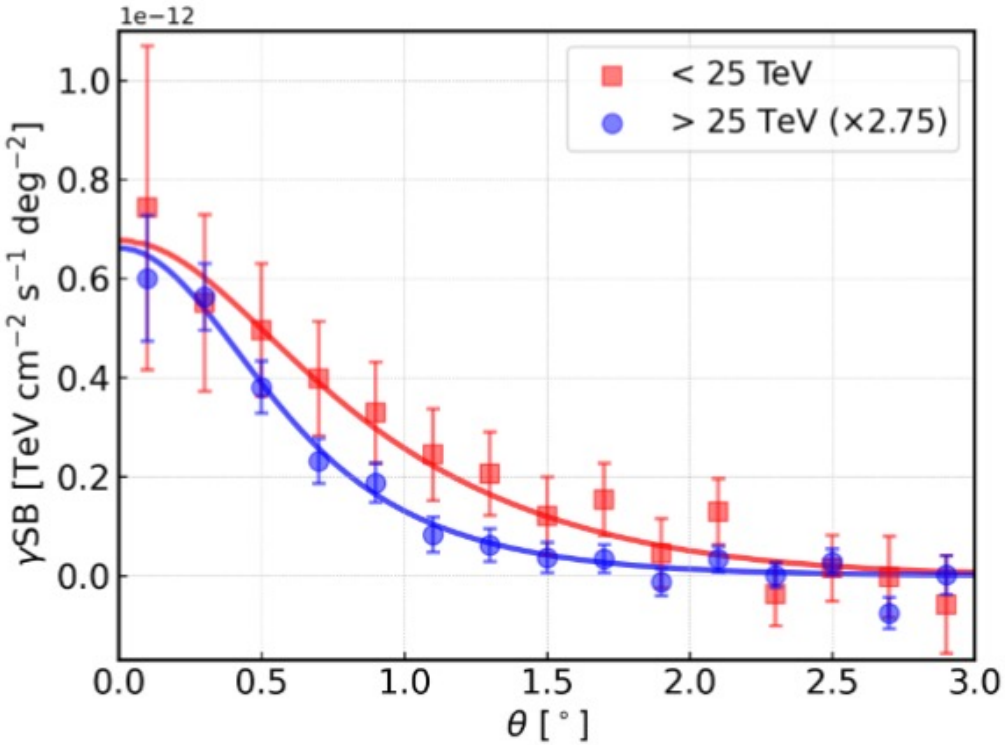

To pulsar:

$\Delta_{\theta\_WCDA} = 0.31°$

$\Delta_{\theta\_KM2A} = 0.23°$

The natural radius of J0635 is approximately $35.3(d/1.35\ kpc)(\theta_d/1.5°)$ pc

Diffusion coefficient as $D(100TeV) = 3.8 \pm 1.0 \times 10^{27}$ erg cm^2 s^{-1} , similar to Geminga halo ($4.5 \pm 1.2 \times 10^{27}$ erg cm^2 s^{-1})

Energy conversion efficiency $\eta = (1.5 \pm 0.2)\% \times (d/1.35pc)^2 \ll 1$

Multi-wavelength comparison

- GeV observation by Fermi-LAT

We carried our data analysis in the off-peak of PSR J0633+0632.
(0.1-300 GeV, 2008-08-04—20230-08-30)

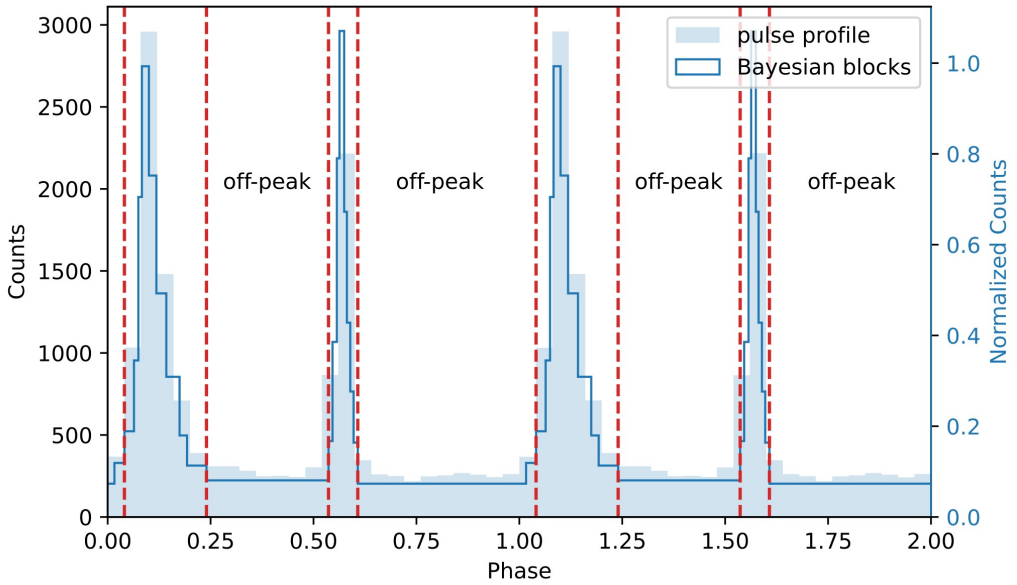

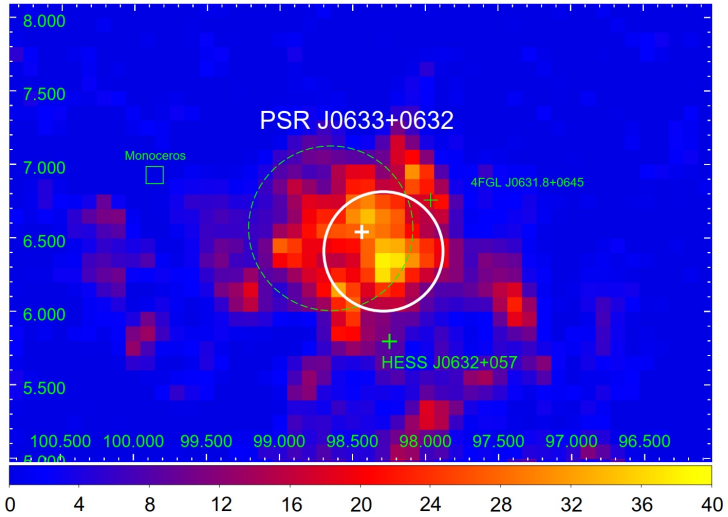

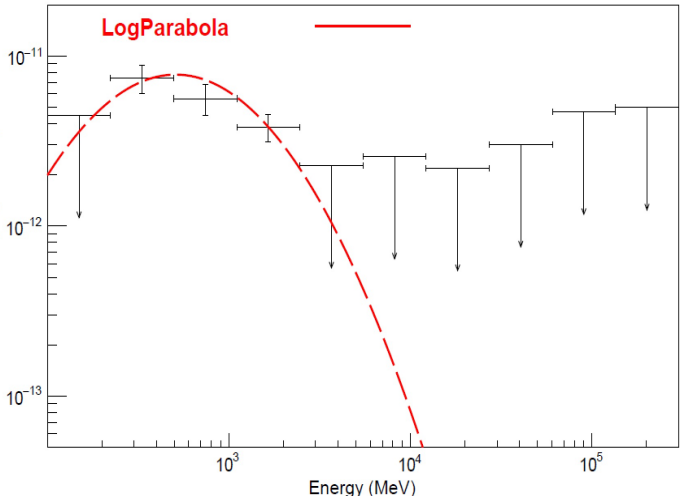

An extended GeV source is detected at the position of PSR J0633+0632,
Gaussian with a sigma of 0.41+/-0.11 degree
TS=106, TS_{ext}=40

Multi-wavelength comparison

- X ray observation

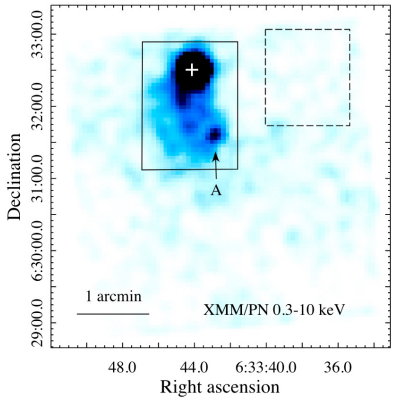

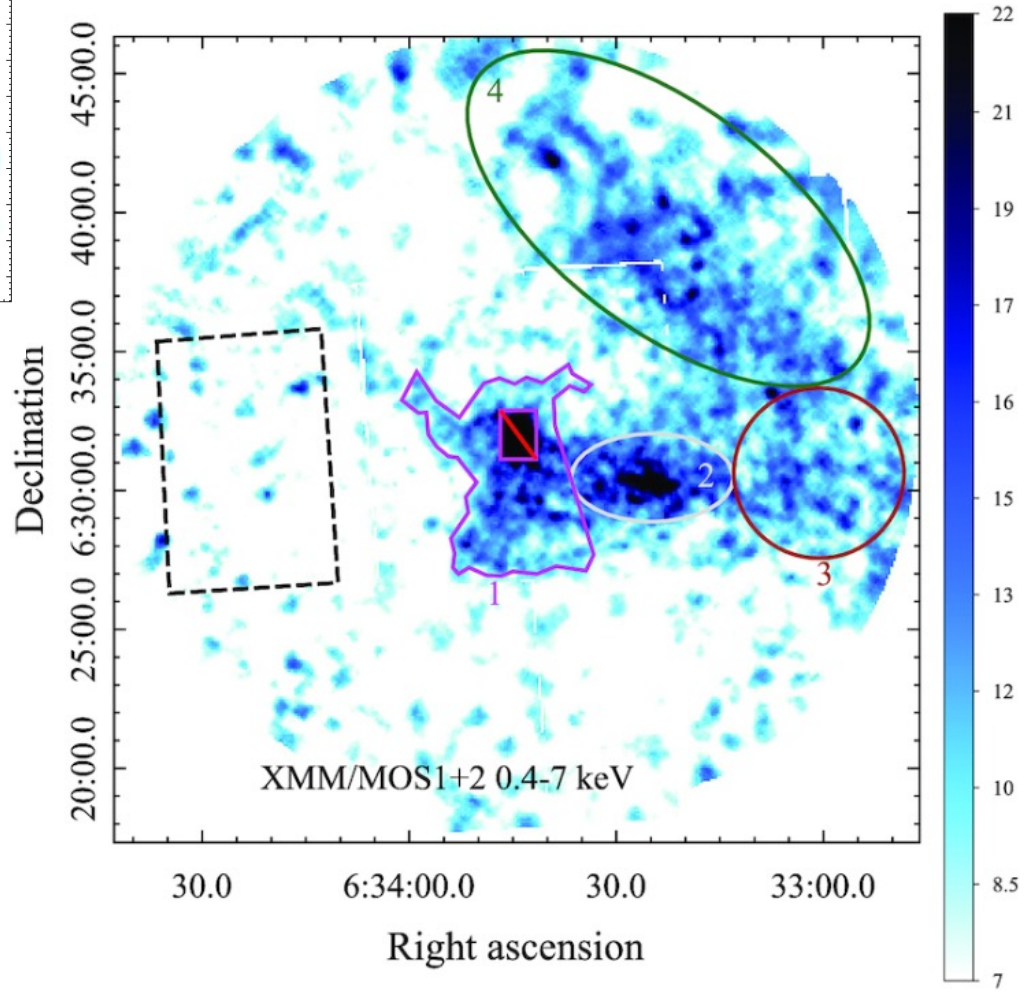

A. Danilenko et al, 2020

Region around PSR J0633+0632 was observed by XMM, revealing

1. the PWN associated with PSR J0633+0632

2.diffuse non-thermal X-ray emission

Multi-wavelength comparison

- Molecular clouds are identified at the direction of J0635 with consistent distance

(MWISP 12CO 0-15 km/s,~1kpc)

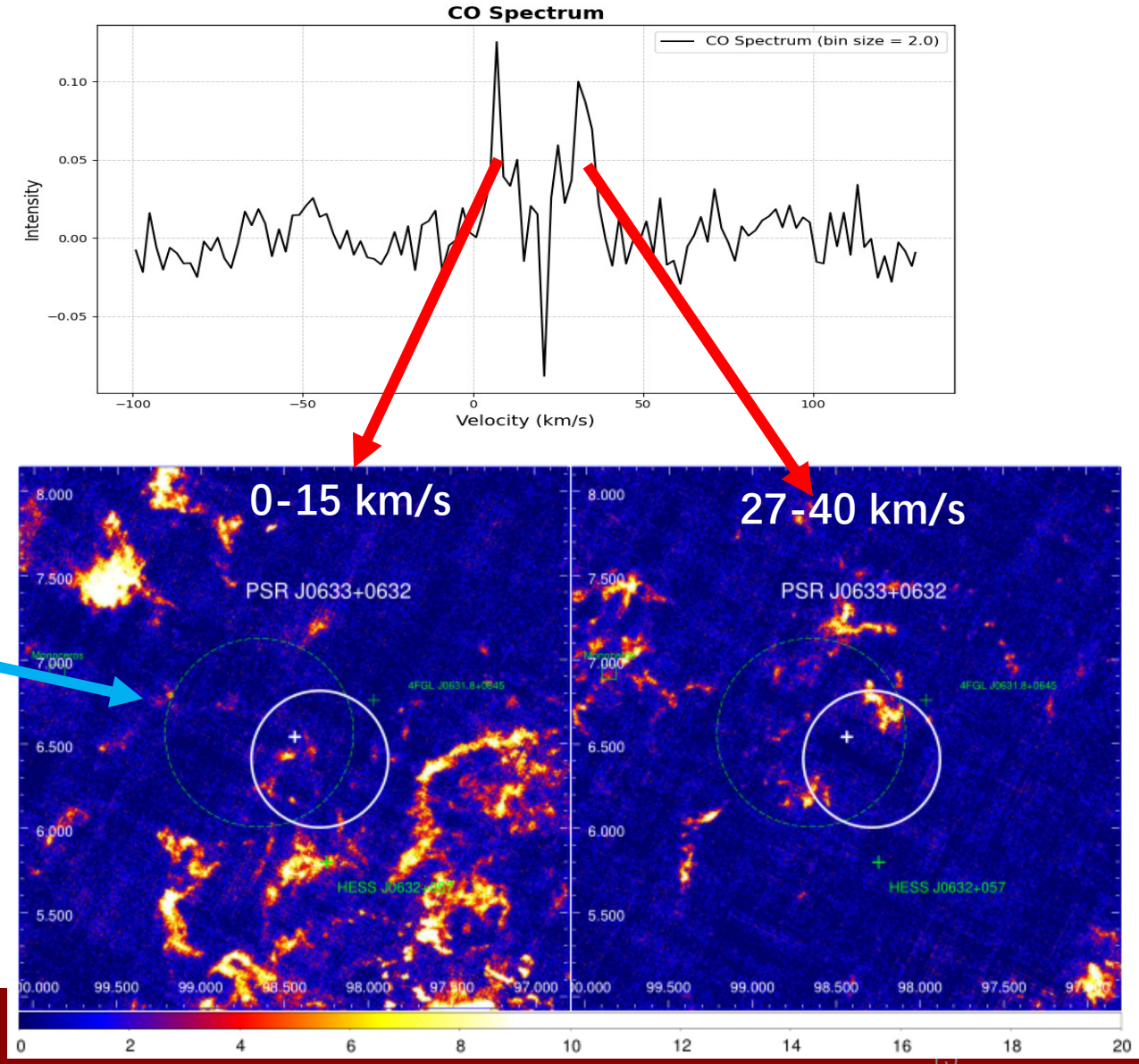

Multi-wavelength comparison

- Atomic clouds are identified at the direction of J0635 with consistent distance

(GALFA HI 0-15 km/s, ~1kpc)

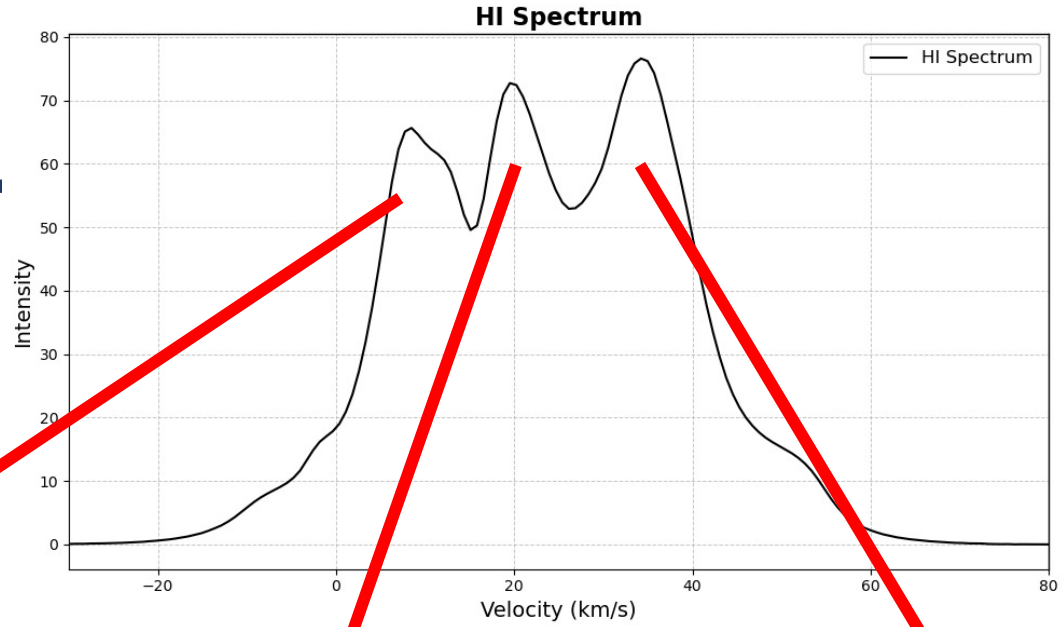

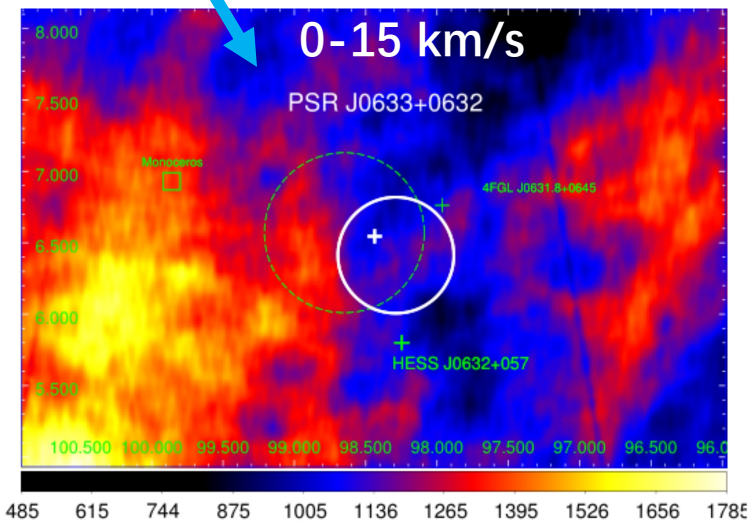

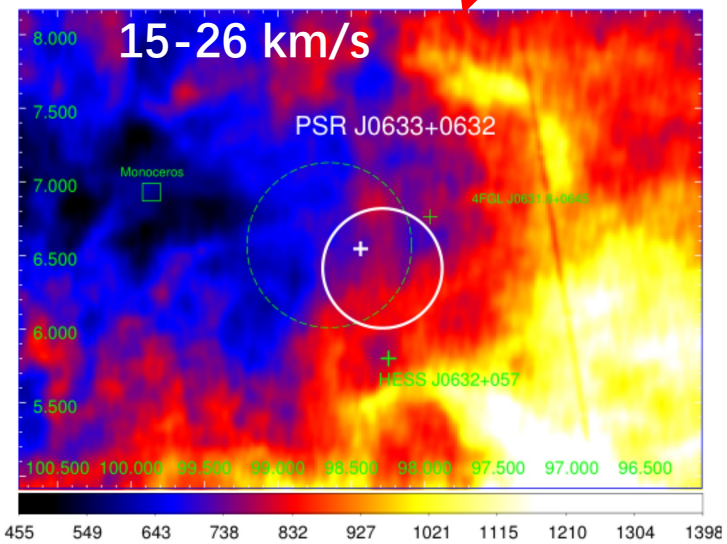

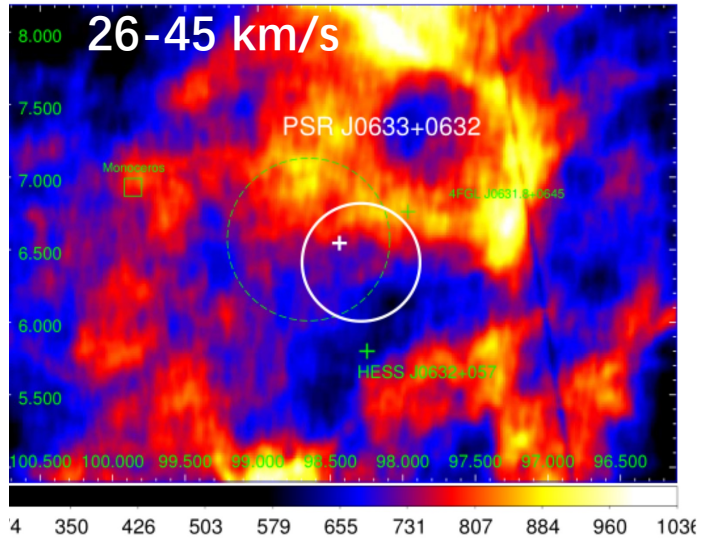

Multi-wavelength comparison

- SED fitting

The spectra from LHAASO and Fermi-LAT both exhibit pronounced curvature features.

Fermi-LAT :

- The spectral shape is consistent with the characteristic π^0-decay bump produced by pp collisions.
- only need two free parameters.
- spectral index is ≈ 3, consistent with an aging SNR with diminished acceleration ability.
- required total proton energy is 5×10^{47} erg, only 0.05% of the initial kinetic energy of a typical supernova explosion.

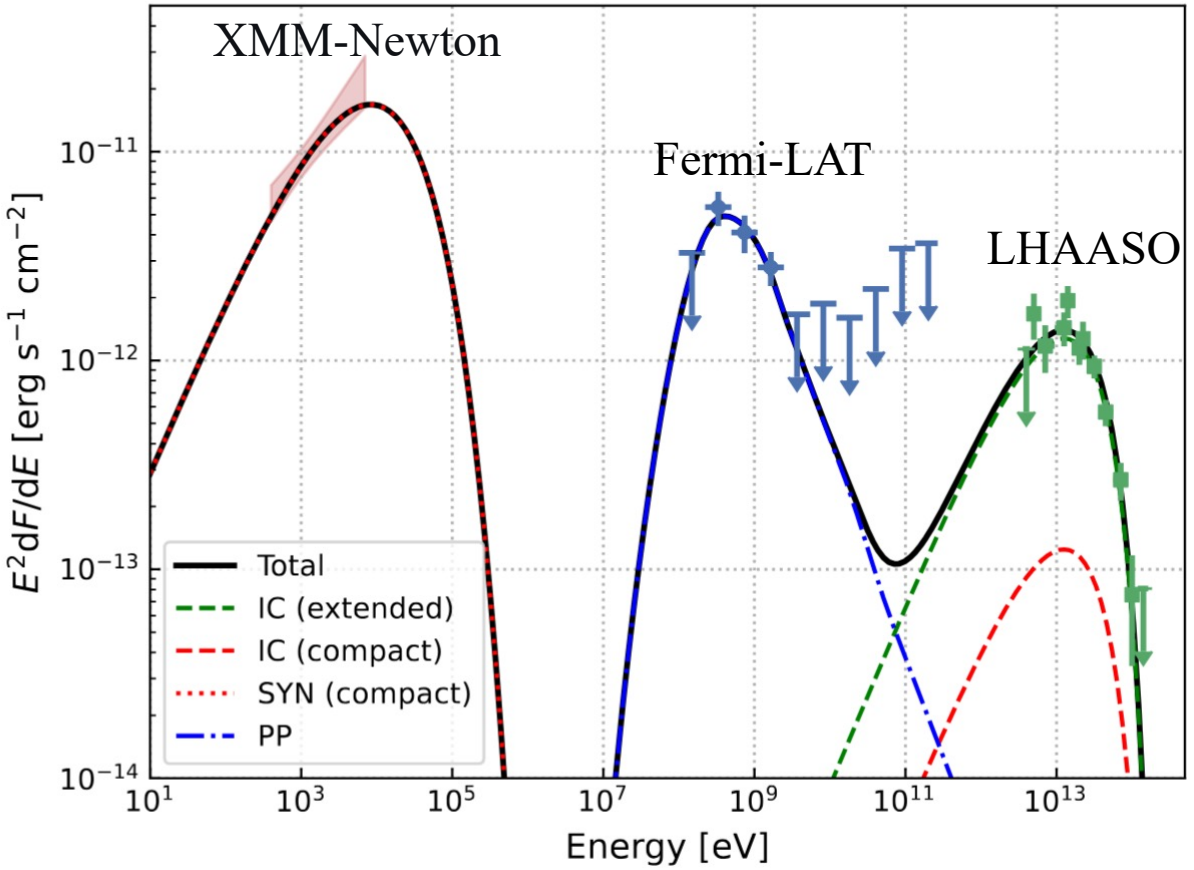

Multi-wavelength comparison

For X-ray and LHAASO

- Extended and compact electron components in the model represent electrons escaping from the PWN into the ISM.

- Compact component generates substantial X-ray flux, its electron population is too small to make a significant contribution to TeV γ rays.

A self-consistent picture emerges :

- high-energy electrons escaping from the PWN propagate partly through regions of a relatively weak turbulent magnetic field, producing the extended γ-ray halo; another fraction encounters the magnetic-field amplification region, generating synchrotron emission with a V-like morphology

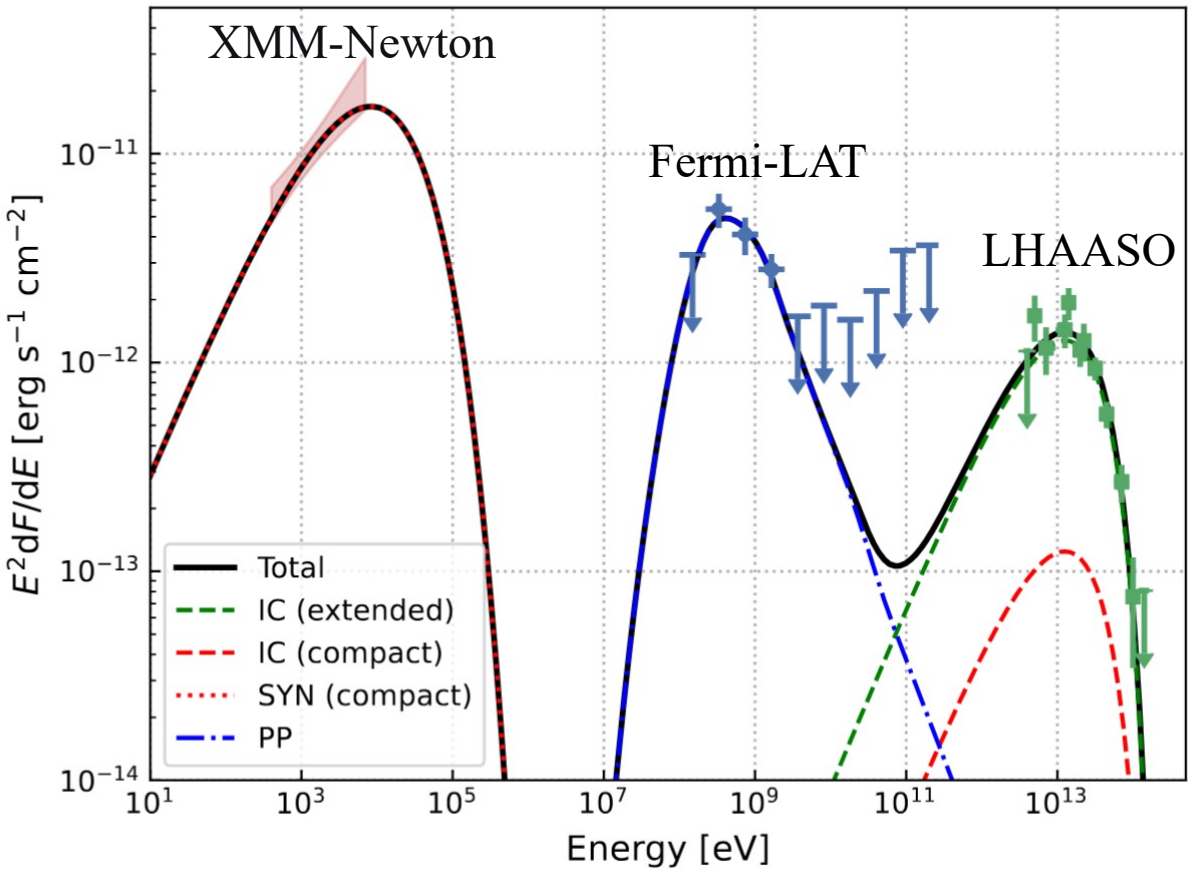

Multi-wavelength comparison

1LHAASO J0635+0619 is a TeV pulsar halo candidate with high possibility (ΔAIC=-7.36 over Gaussian).

It is among the youngest pulsar halo (59 kyr).

It is the second one within SNR environment and the first one with clear X-ray and GeV counterpart.

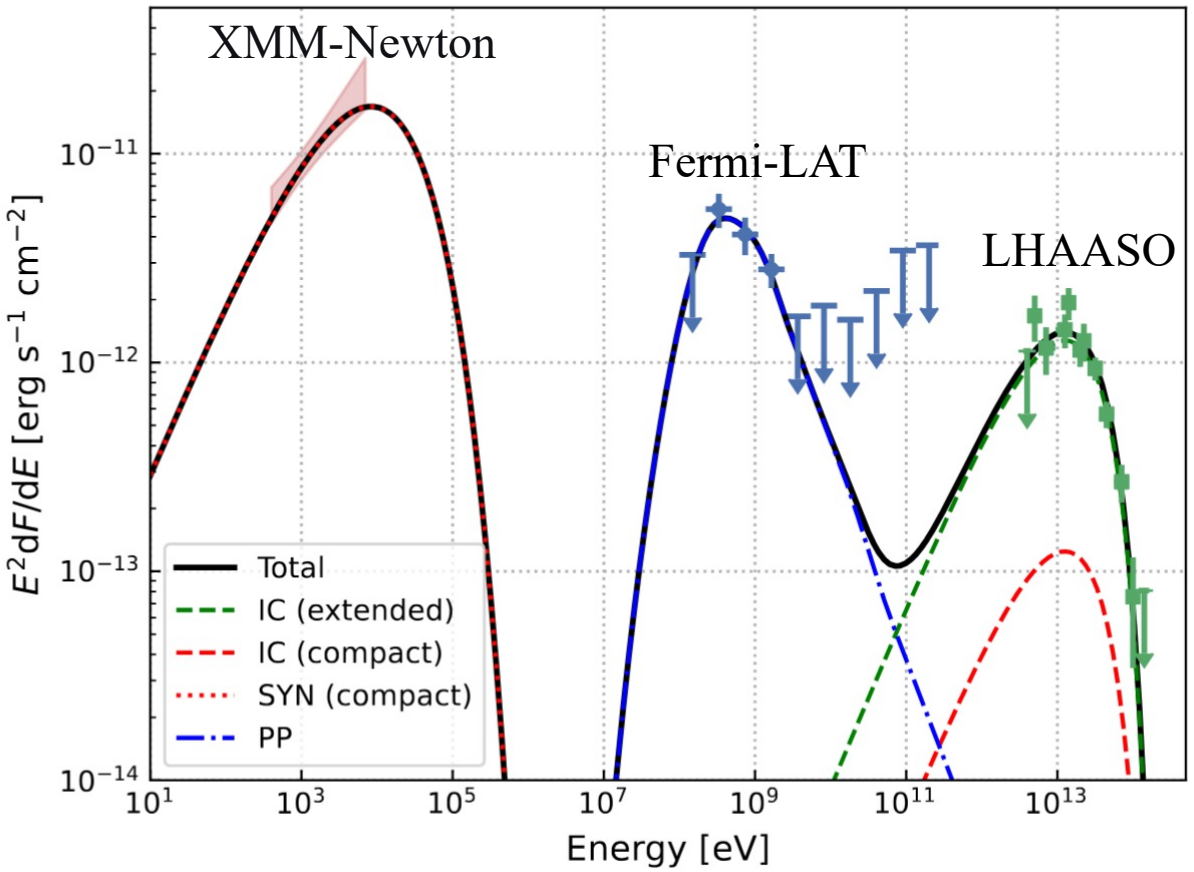

Summary

- J0635 is a TeV pulsar halo candidate with distinct features.
- The diffusion coefficient is consistent with typical values observed in pulsar halos.
- The physical scale is significantly larger than that of the PWN.
- The diffuse X-ray emission is consistent with a leptonic origin.
- Molecular and atomic cloud observations support a hardonic origin for GeV.

Thanks for listening !

About binary

HESS J0632+057

- Type: TeV gamma-ray binary (TGB)
- Compact object: naturally neutron star
- Companion star: Be star
- Orbital period: ~317d
- Eccentricity: ~0.45

We have, for the first time, presented the energy spectrum of the binary above TeV band.

$$\frac{\mathrm{d}N}{\mathrm{d}E} = 1.32\times10^{-16}\ \mathrm{TeV\ cm^{-1}\ s^{-1}}\left(\frac{E}{20\ \mathrm{TeV}}\right)^{-2.82}$$

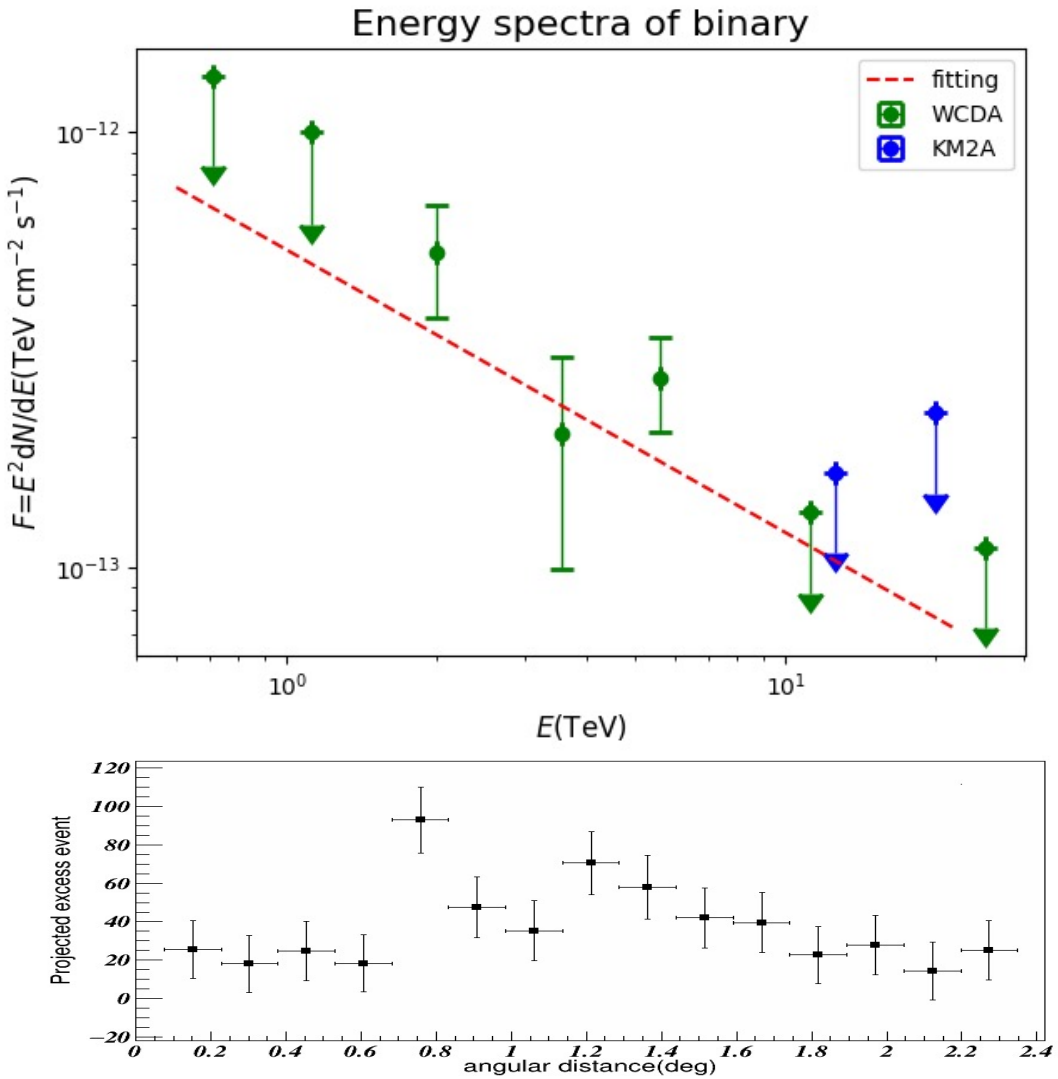

Multi-wavelength comparison

- TeV Gamma ray observation

From 3HWC Catalog:
3HWC J0634+067 – a potential TeV halo around the pulsar PSR J0633+0632.

position of RA = 98.66°, Dec = 6.73°
Index : $2.27 \pm 0.10\ ^{+0.09}_{-0.11}$

Differential flux at 7 TeV is:
$9.0^{+1.3\ +2.7}_{-1.4\ -1.2} \times 10^{-15}$ erg cm^{-2} s^{-1}

Energy Range: 7.6 TeV − 171.1 TeV

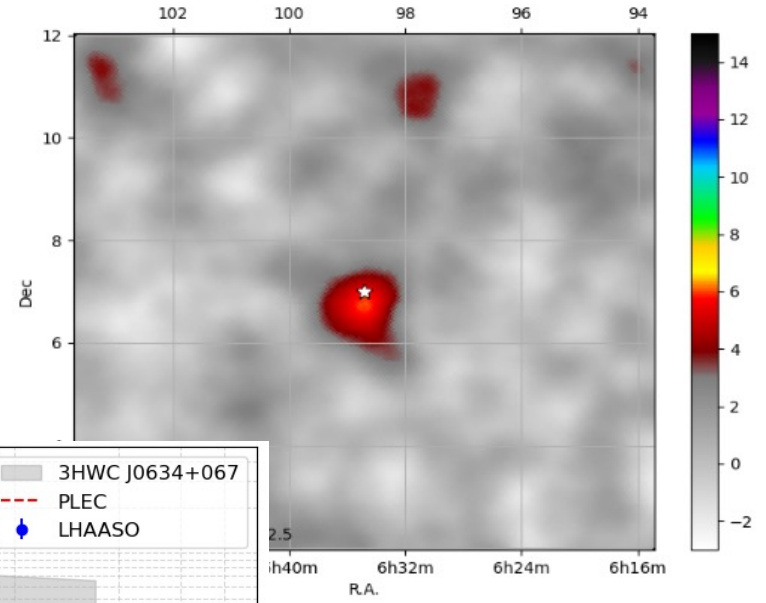

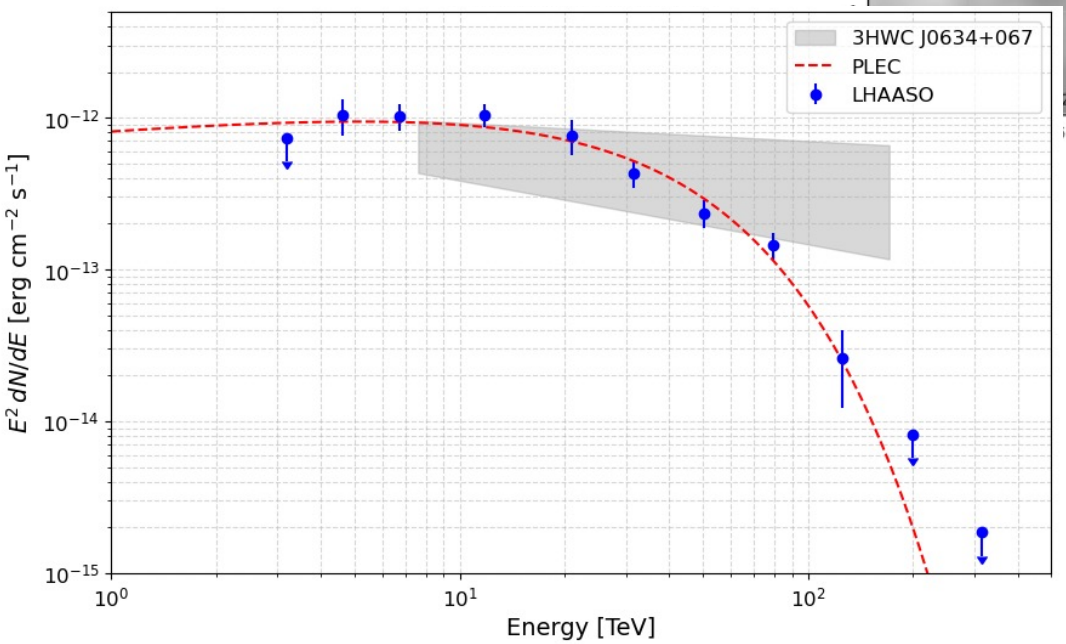

Multi-wavelength comparison

- X ray observation

XMM-Newton
The PWN was observed by XMM-Newton, extending approximately 1 arcmin

V-like Non-thermal region
relativistic electrons
Monoceros Loop :

- shock velocity may be ~ 300 km s^{-1}
- Assuming a magnetic field of 10 μG
- the maximum energy attainable by electrons accelerated at the present shock is limited to ~ 5 TeV

The electron energies required to explain the XMM-Newton observations approach 100 TeV

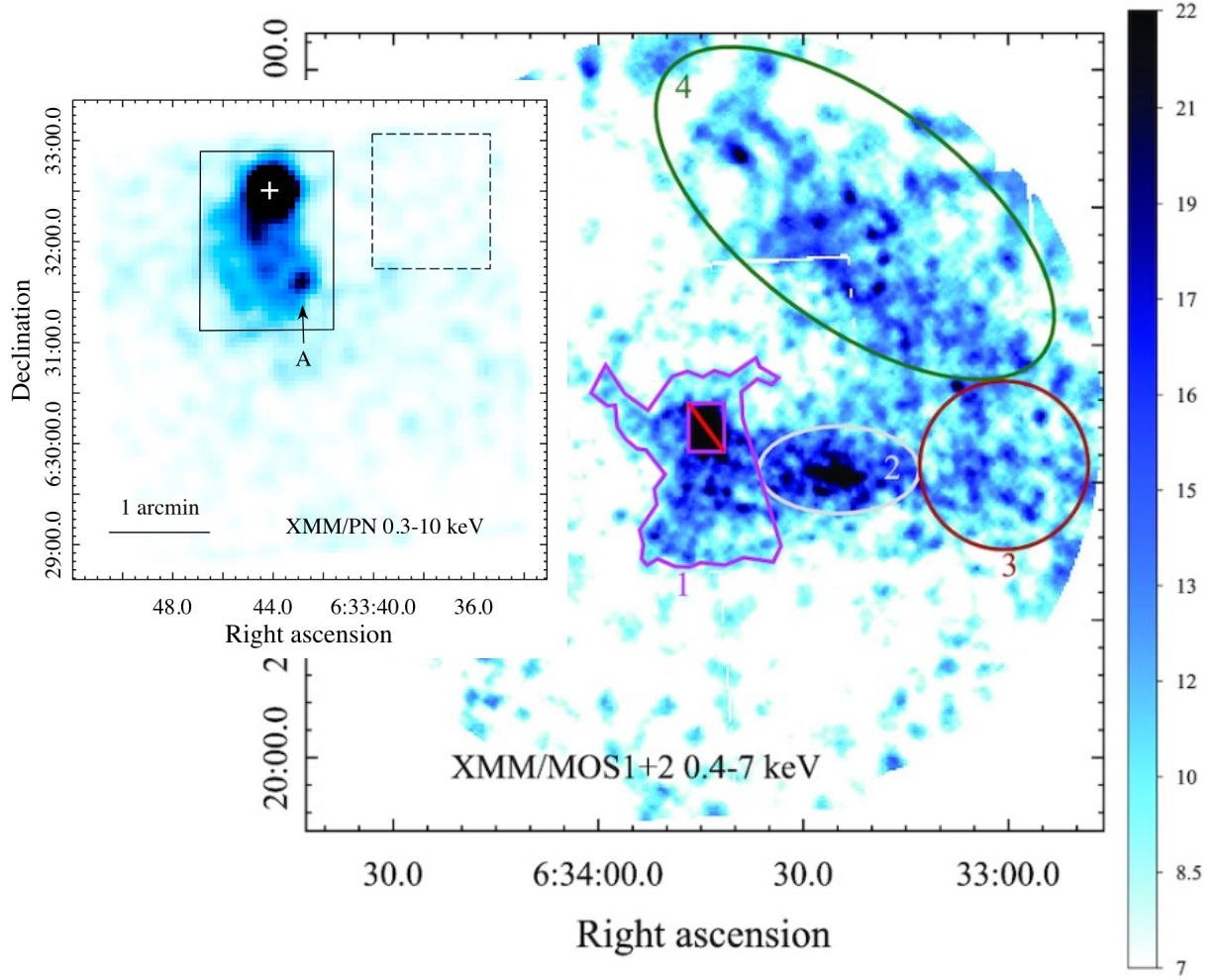

A. Danilenko et al, 2020

Systematic error analysis

We separately evaluated the effects of Galactic diffuse emission on the observations.

The maximum effect on the spectral points is about 23%.

$$\frac{\mathrm{d}N}{\mathrm{d}E} = 8.92\times10^{-15}\ \mathrm{TeV\ cm^{-1}\ s^{-1}} \left(\frac{E}{50\ \mathrm{TeV}}\right)^{-2.80}$$

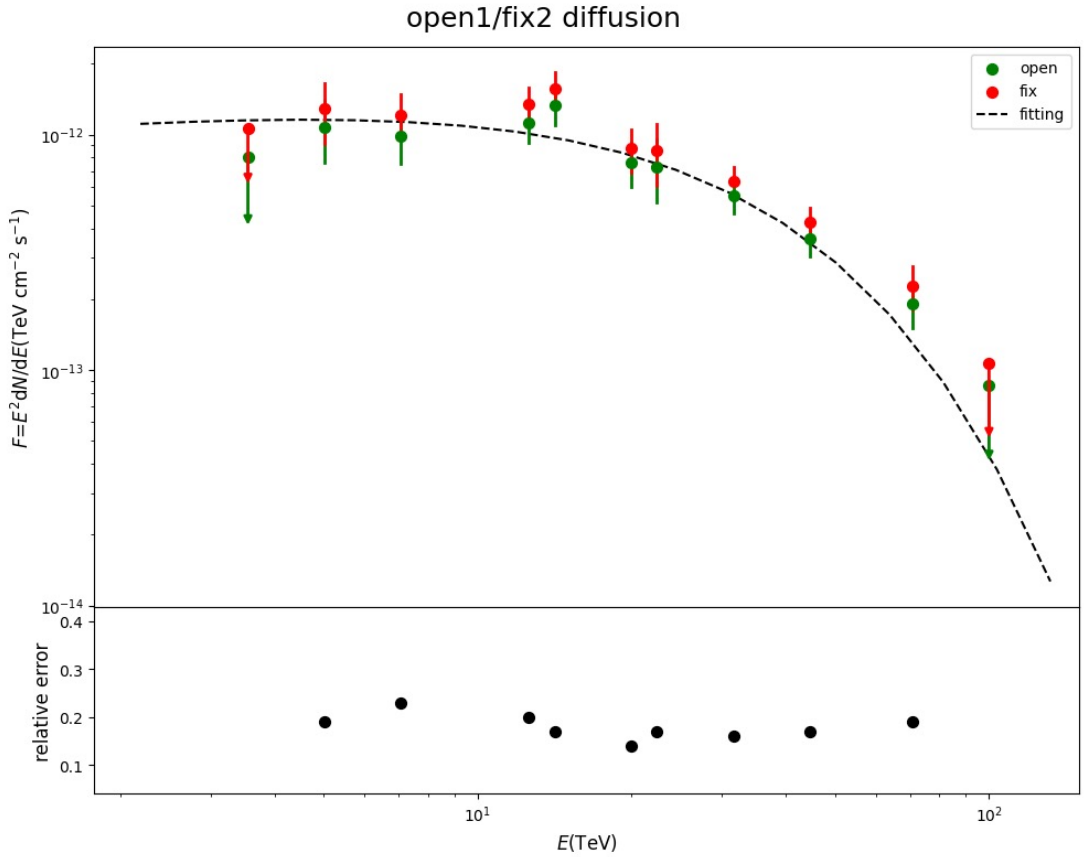

Data Analysis and Results

Given the diffuse characteristics of the WCDA sky map, we speculate that there may be more than one radiation source contributing to the emission within the target region.

WCDA	**RA (°)**	**Dec (°)**	σ (°)	ΔTS
1 source	98.54 ± 0.08	6.42 ± 0.09	0.66 ± 0.08	0
2 Sources*	98.69 ± 0.11	6.66 ± 0.10	0.64 ± 0.10	40.48
	98.28 ± 0.04	5.80 ± 0.07	None	
3 Sources	98.68 ± 0.10	6.66 ± 0.10	0.64 ± 0.08	
	98.28 ± 0.05	5.79 ± 0.04	None	52.15
	100.47 ± 0.07	7.45 ± 0.07	None	
KM2A	**RA (°)**	**Dec (°)**	σ (°)	ΔTS
1 source*	98.67 ± 0.06	6.52 ± 0.06	0.52 ± 0.07	0
2 Sources	98.69 ± 0.02	6.52 ± 0.06	0.48 ± 0.06	9.63
	99.95 ± 0.09	6.37 ± 0.07	None	

PSR J0633+0632
RA : 98.43°
Dec : 6.54°

To pulsar:

$\Delta_{\theta\_WCDA} = 0.31°$

$\Delta_{\theta\_KM2A} = 0.23°$

Systematic error analysis

We performed statistical analysis on the residuals of the fitting results.

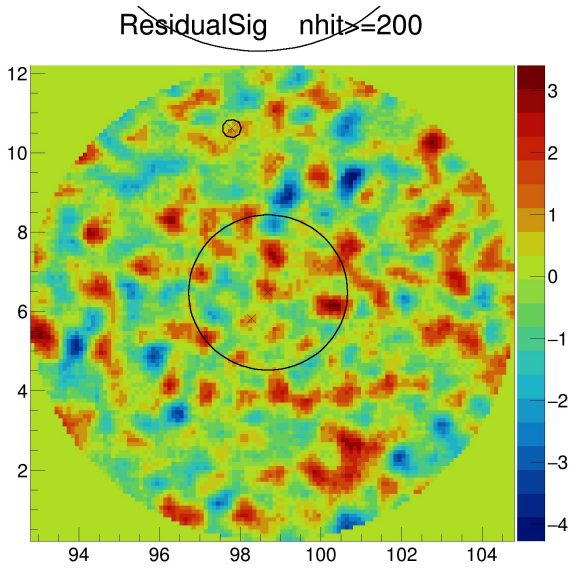

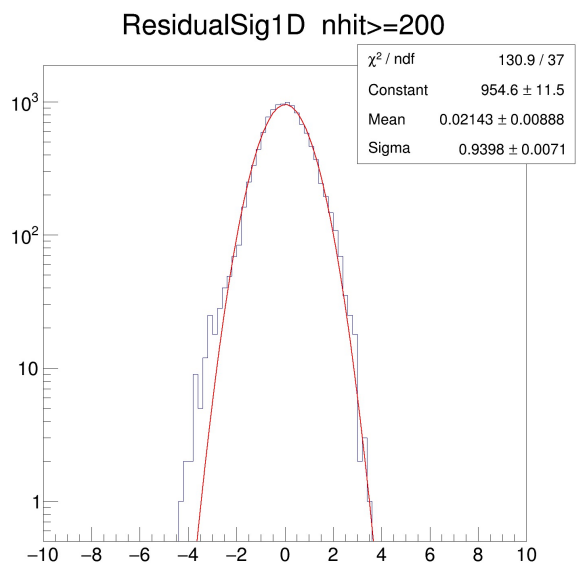

wcda

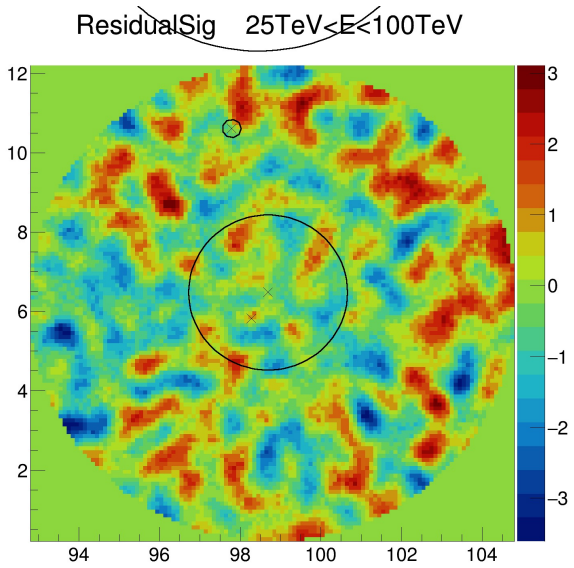

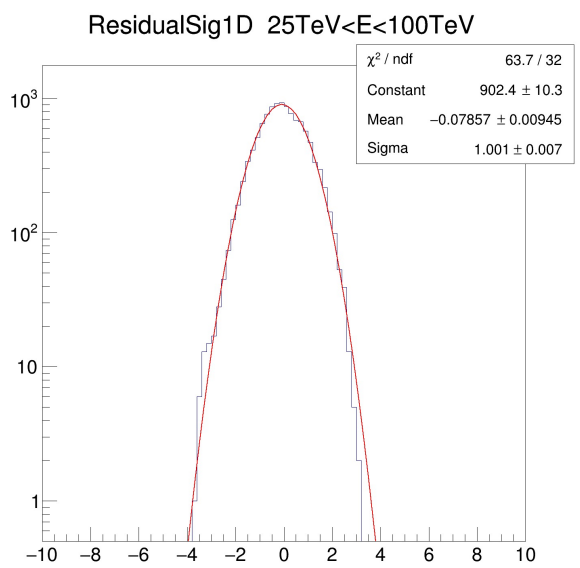

km2a

Cross check

	RA	DEC	THEAT_D	NORM (1e-14)	CUT	ALPHA
result	98.67° ± 0.05°	6.48° ±0.05°	1.50° ± 0.17°	1.07 ± 0.19	25.00 ± 5.29	1.81 ± 0.19
crosscheck	98.69° ± 0.07°	6.49° ±0.06°	1.82° ± 0.24°	1.27 ± 0.28	28.60 ± 7.27	1.82 ± 0.23

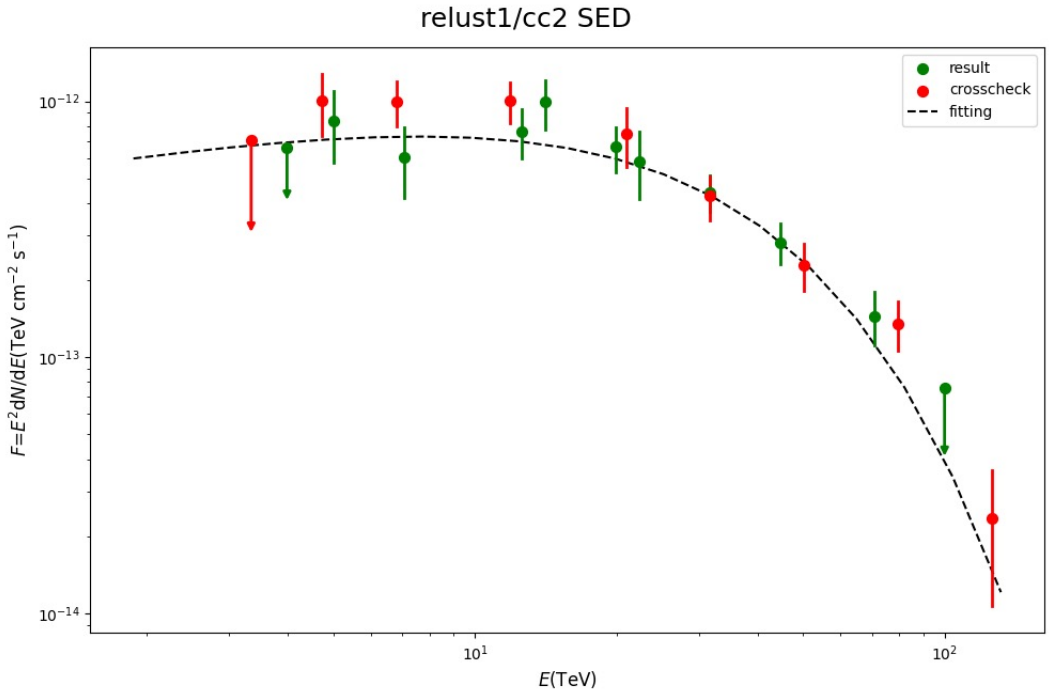

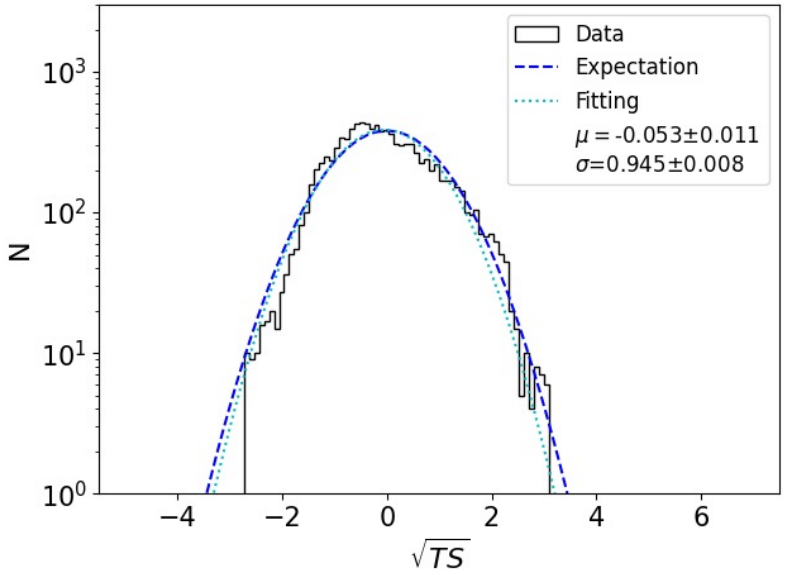
Data
Expectation
Fitting
μ = -0.053±0.011
σ=0.945±0.008
N
$\sqrt{TS}$

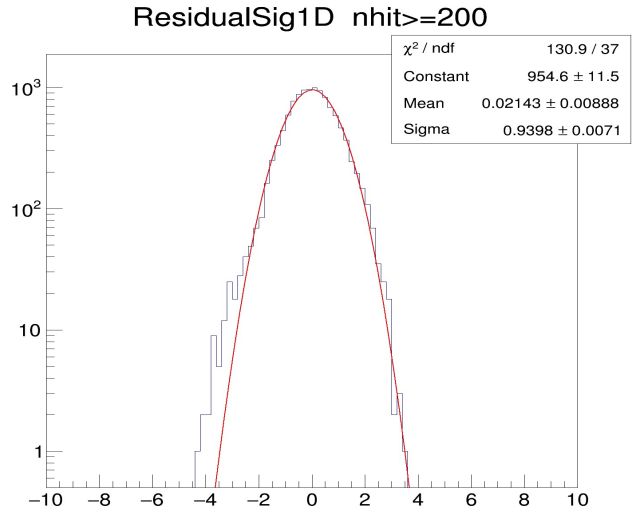
ResidualSig1D nhit>=200
χ^2 / ndf 130.9 / 37
Constant 954.6 ± 11.5
Mean 0.02143 ± 0.00888
Sigma 0.9398 ± 0.0071

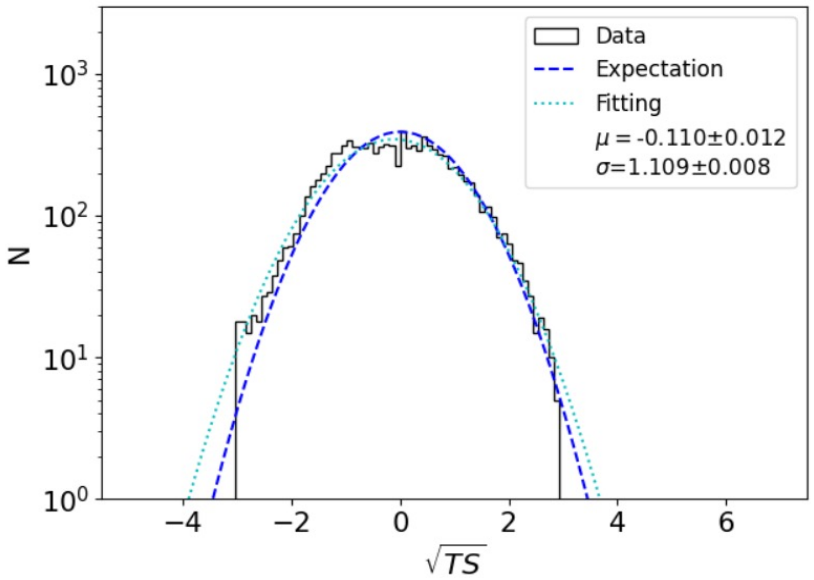
Data
Expectation
Fitting
μ = -0.110±0.012
σ=1.109±0.008
N
$\sqrt{TS}$

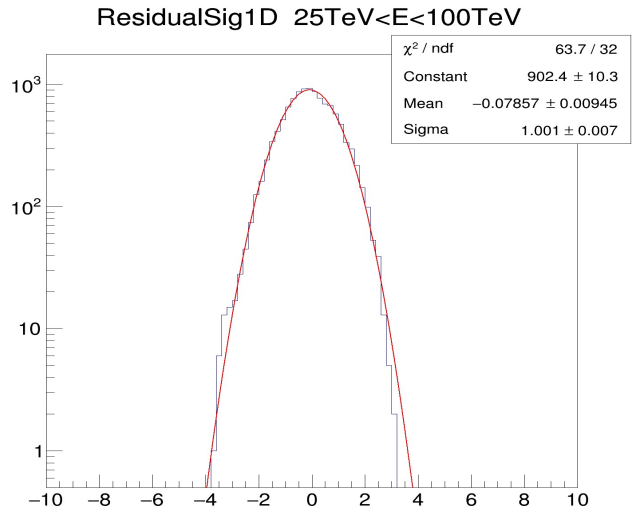
ResidualSig1D 25TeV<E<100TeV
χ^2 / ndf 63.7 / 32
Constant 902.4 ± 10.3
Mean −0.07857 ± 0.00945
Sigma 1.001 ± 0.007

Multi-wavelength comparison

- X ray observation

The PWN was observed by XMM-Newton, extending approximately 2 arcminutes, exhibiting a flux of 1.12×10^{-13}erg cm^{-2} s^{-1} from 2 keV to 10 keV, with a corresponding luminosity of 1.25×10^{31} erg s^{-1}.

eROSITA also observed the vicinity of pulsar J0633+0632 in the energy range of 0.2 keV to 8 keV, but no diffuse emission was detected within the 1° region.

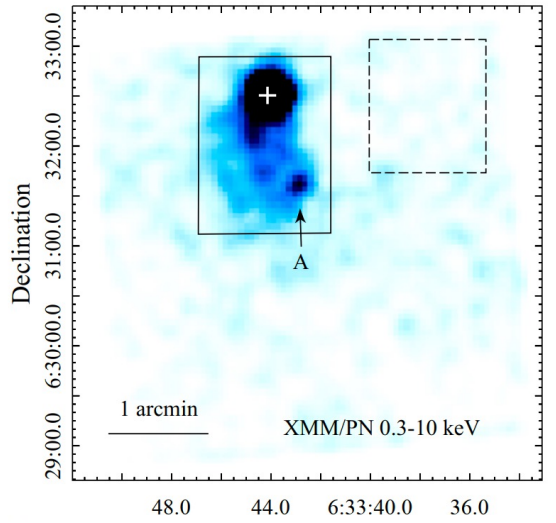

A. Danilenko et al, 2020

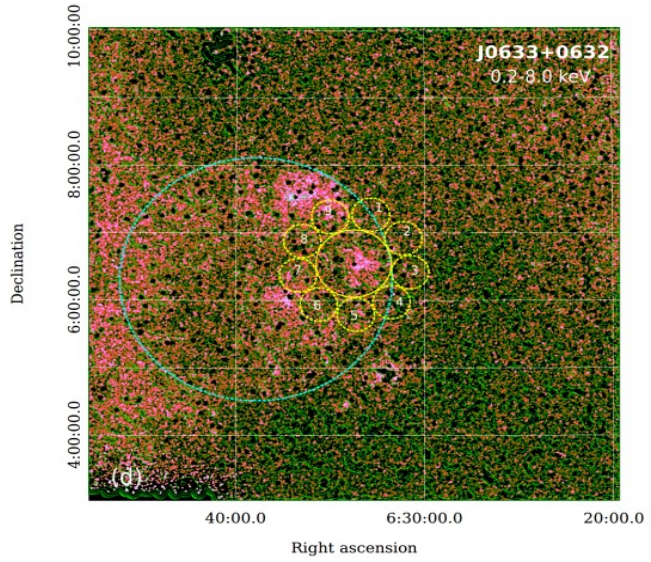

A. Khokhriakova et al, 2023